JOURNAL OF GUIDANCE, CONTROL, AND DYNAMICS
Vol. 26, No. 4, July–August 2003

Technique for Escape from Geosynchronous Transfer Orbit Using a Solar Sail

Victoria L. Coverstone* and John E. Prussing†
University of Illinois at Urbana–Champaign, Urbana, Illinois 61801

A technique for escaping the Earth using a solar sail is developed and numerically simulated. The spacecraft is initially in a geosynchronous transfer orbit (GTO). A sail force control algorithm is derived that continuously orients the sail in three dimensions to maximize the component of sail force along the velocity vector. This approach maximizes the instantaneous rate of increase of the total orbital energy. Trajectories using this strategy are not necessarily minimum-time solutions, but independent analysis has shown that for the realistic order of magnitude of sail acceleration considered here, the solutions obtained are near-minimum-time trajectories. The equations of motion for the trajectory are expressed in modified equinoctial orbital elements, which are well behaved as the trajectory goes from elliptic to hyperbolic during escape. In this preliminary study a spherical gravity model for the Earth is assumed. The gravitational perturbation of the sun is included but atmospheric drag and shadowing effects of the Earth are neglected. No sail angle, sail angle rate, or minimum perigee radius constraints are included. Numerical results confirm that escape does occur, with the escape time highly dependent on the sail acceleration magnitude but relatively independent of the time of year of the deployment.

Introduction

AN important recent publication on solar sailing is a book by McInnes,[1] which provides a large number of references on the topic. The concept of solar sailing dates back to the 1920s in the work of the Soviet pioneers in astronautics, Tsiolkovsky[2,3] and Tsander (Ref. 4, quoting from a 1924 report by the author). Following a dormant period, the subject received renewed interest in the 1950s and 1960s (Refs. 5–10). These publications were followed by numerous studies from the 1970s up to the present.[11–38] The first major mission design study of the concept was in 1976–1978 for a proposed Halley's comet rendezvous mission.[19]

This paper is a preliminary study of the feasibility of escaping from Earth using a solar sail that is initially in a geosynchronous transfer orbit (GTO). A spherical gravity model for the Earth is assumed, and solar gravitational perturbation is included. Atmospheric drag and shadowing effects of the Earth are neglected. No sail angle, sail angle rate, or minimum perigee radius constraints are included.

The concept of using a solar sail for Earth escape was investigated in the 1960s by Sands[7] and Fimple.[8] In these analyses an initial circular orbit was used, and simplifying assumptions were made such as a fixed direction of the sun and special initial inclinations. More recent studies on escape include Uphoff,[13] Sackett and Edelbaum,[14] and Green.[15]

Orbit Geometry and Solar Sail Acceleration

The reference orbit plane is the ecliptic, and the coordinate axis definitions and geometry are shown in Fig. 1. The XYZ axes are sun-centered inertial axes with the X axis directed to the first point in Aries, as shown. The $\alpha\beta$ axes are Earth centered and in the ecliptic plane. These axes rotate with the apparent motion of the sun, so that the α axis is always directed from the Earth to the sun.

Received 7 March 2000; revision received 27 February 2003; accepted for publication 7 March 2003.

*Associate Professor, Department of Aeronautical and Astronautical Engineering, 306 Talbot Laboratory. Associate Fellow AIAA.

†Professor, Department of Aeronautical and Astronautical Engineering, 306 Talbot Laboratory. Fellow AIAA.

The acceleration (force per unit mass) on a flat sail is given in Ref. 1 as

$$\boldsymbol{S} = (2WA/mc)(\boldsymbol{n}^T\hat{\boldsymbol{\alpha}})^2\boldsymbol{n} = S_0(\boldsymbol{n}^T\hat{\boldsymbol{\alpha}})^2\boldsymbol{n} \tag{1}$$

where W is the (constant) solar intensity at 1 astronautical unit (AU) from the sun, A is the sail area, c is the speed of light in a vacuum, $\boldsymbol{n}$ is the unit vector normal to the sail, and $\hat{\boldsymbol{\alpha}}$ is a unit vector in the direction of the sun. The constant S_0 is the characteristic acceleration of the sail at 1 AU. The squared term in Eq. (1) represents the variation in the sail acceleration according to the square of the cosine of the angle between the sail normal and the direction of the sun.

For the ideal sail assumed, the sail force is normal to the sail, but in a nonideal sail, this may not be true due to imperfect reflectivity and sail billowing. In addition, a realistic sail can have a maximum cone angle (the angle between the photon stream and the sail force) of approximately 55 deg, rather than the 90 deg for an ideal sail.[33] Also, the 6% variation in the magnitude of the solar flux due to the eccentricity of the Earth's orbit is not included. Studies beyond this preliminary analysis would need to include these and other effects.

Maximum Orbital Energy Rate

To escape the Earth, an efficient method must be devised to increase the total orbital energy. The spacecraft equations of motion are

$$\dot{\boldsymbol{r}} = \boldsymbol{v} \tag{2}$$

$$\dot{\boldsymbol{v}} = \boldsymbol{g}_c(\boldsymbol{r}) + \boldsymbol{\Delta} \tag{3}$$

where $\boldsymbol{r}$ and $\boldsymbol{v}$ are the position and velocity vectors of the spacecraft relative to the center of the central body (Earth), $\boldsymbol{g}_c(\boldsymbol{r})$ is the gravitational acceleration of the central body, and $\boldsymbol{\Delta}$ is the total disturbing acceleration. In this study, the total disturbing acceleration is the sum of the solar sail acceleration $\boldsymbol{S}$ and the gravitational perturbation of the third body (sun) $\boldsymbol{g}_p$:

$$\boldsymbol{\Delta} = \boldsymbol{S} + \boldsymbol{g}_p \tag{4}$$

The disturbing function for the third-body perturbation is given by Battin.[39]

The orbital energy is given by $E = \frac{1}{2}\boldsymbol{v}^T\boldsymbol{v} + U(\boldsymbol{r})$, where $U(\boldsymbol{r})$ is the potential energy per unit mass for the gravitational field of the central body. The time rate of change of the orbital energy is

$$\dot{E} = \dot{\boldsymbol{v}}^T\boldsymbol{v} + \dot{U} = \dot{\boldsymbol{v}}^T\boldsymbol{v} + \frac{\partial U}{\partial \boldsymbol{r}}\dot{\boldsymbol{r}} \tag{5}$$

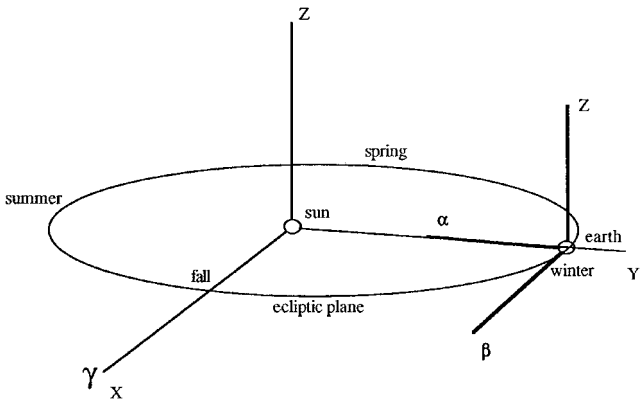

Fig. 1 Axis definitions: *XYZ* are inertial, $\alpha\beta Z$ rotate with sun direction.

When Eqs. (2) and (3) are used and because $\boldsymbol{g}_c^T = -\partial U/\partial \boldsymbol{r}$,

$$\dot{E} = (\boldsymbol{g}_c + \boldsymbol{\Delta})^T \boldsymbol{v} - \boldsymbol{g}_c^T \boldsymbol{v} = \boldsymbol{\Delta}^T \boldsymbol{v} = \boldsymbol{S}^T \boldsymbol{v} + \boldsymbol{g}_p^T \boldsymbol{v} \tag{6}$$

A simple control strategy to efficiently increase the orbital energy is to maximize the instantaneous rate of energy change in Eq. (6) by orienting the sail to maximize $\boldsymbol{S}^T\boldsymbol{v}$. The derivation of a control law to realize this is given in the Appendix. To implement this control law, the sail must be continuously oriented to maximize the component of the sail acceleration given in Eq. (1) along the instantaneous velocity vector at each point along the trajectory. Note that this "greedy" method is not necessarily equivalent to minimizing the time to achieve a specific final energy (such as escape) because the performance index is a functional that depends on the entire trajectory and control history. However, the required sail orientation for the greedy method is simpler to implement because it is based on current data. Results of a recent study by Hartmann[40] that determines minimum-time solutions using direct transcription and collocation indicate that for low sail accelerations of the magnitude in this paper (1 mm/s$^2 \approx 10^{-4}g$), the trajectories using the greedy method are near-minimum-time solutions. However, for large sail accelerations ($10^{-2}g$), the actual minimum times are less. (This large sail acceleration is unrealistic for Earth-orbiting solar sails, but it is applicable for orbits about a much smaller central body, such as an asteroid, or about a libration point.) It is also true that having the actual minimum-time trajectory may not be a critical issue because propellant mass is not being consumed.

Sackett and Edelbaum[14] and Green[15] investigated minimum-time solar sail trajectories to achieve a specified energy increase. In Ref. 14, a rapid rise in eccentricity is reported that can cause the perigee radius to drop below the Earth's surface. A similar effect was evident in some of the solutions obtained in the current study.

Modified Equinoctial Orbital Elements

In the process of escaping the Earth, the spacecraft trajectory goes from an initial elliptic orbit (eccentricity $e < 1$), through parabolic orbit ($e = 1$), to a hyperbolic orbit ($e > 1$). The standard set of equinoctial orbital elements does not accommodate orbits with $e \geq 1$. To remedy this, a set of modified equinoctial orbital elements is described by Betts[41] based on a derivation by Walker et al.[42]

In terms of classical orbital elements the modified equinoctial elements are[41]

$$p = a(1 - e^2) \tag{7}$$

$$f = e\cos(\omega + \Omega) \tag{8}$$

$$g = e\sin(\omega + \Omega) \tag{9}$$

$$h = \tan(i/2)\cos\Omega \tag{10}$$

$$k = \tan(i/2)\sin\Omega \tag{11}$$

$$L = \Omega + \omega + \nu \tag{12}$$

where the usual terminology applies: p is the semilatus rectum (parameter), a the semimajor axis, e the eccentricity, ω the argument of periapse, Ω the longitude of ascending node, i the inclination, L the true longitude, and ν the true anomaly.

A convenient coordinate frame to express the components of the disturbing acceleration is described by the local radial, tangential, normal RTH coordinate frame unit vectors:

$$\hat{\boldsymbol{r}} \equiv \boldsymbol{r}/r \tag{13}$$

$$\hat{\boldsymbol{h}} \equiv (\boldsymbol{r} \times \boldsymbol{v})/|\boldsymbol{r} \times \boldsymbol{v}| \tag{14}$$

$$\hat{\boldsymbol{t}} \equiv \hat{\boldsymbol{h}} \times \hat{\boldsymbol{r}} \tag{15}$$

The disturbing acceleration can then be expressed in the RTH coordinate frame as

$$\boldsymbol{\Delta} = \Delta_r \hat{\boldsymbol{r}} + \Delta_t \hat{\boldsymbol{t}} + \Delta_h \hat{\boldsymbol{h}} \tag{16}$$

The equations of motion in terms of the modified equinoctial elements are expressed in terms of auxiliary variables:

$$w \equiv 1 + f\cos L + g\sin L \tag{17}$$

$$r \equiv p/w \tag{18}$$

$$s^2 \equiv 1 + h^2 + k^2 \tag{19}$$

as

$$\dot{p} = (2p/w)\sqrt{p/\mu}\,\Delta_t \tag{20}$$

$$\dot{f} = \sqrt{p/\mu}\{\Delta_r \sin L + [(w+1)\cos L + f](\Delta_t/w) - (h\sin L - k\cos L)(g\Delta_h/w)\} \tag{21}$$

$$\dot{g} = \sqrt{p/\mu}\{-\Delta_r \cos L + [(w+1)\sin L + g](\Delta_t/w) + (h\sin L - k\cos L)(f\Delta_h/w)\} \tag{22}$$

$$\dot{h} = \sqrt{p/\mu}\left(s^2\Delta_h/2w\right)\cos L \tag{23}$$

$$\dot{k} = \sqrt{p/\mu}\left(s^2\Delta_h/2w\right)\sin L \tag{24}$$

$$\dot{L} = \sqrt{\mu p}(w/p)^2 + (1/w)\sqrt{p/\mu}(h\sin L - k\cos L)\Delta_h \tag{25}$$

Note that in Eqs. (20–25), when all of the disturbing acceleration components are zero, the first five elements are constant and the rate of change of the sixth element (true longitude) is equal to the angular momentum $\sqrt{(\mu p)}$ divided by the square of the radius [from Eq. (18)], as it should be to conserve orbital angular momentum. In Eq. (20), a typographical error in Ref. 41 is corrected. In Ref. 41, an error in Ref. 42 is corrected, and this correction appears in Eq. (22).

Energy Increase Control Law

As derived in the Appendix, the components of the sail normal vector $\boldsymbol{n}$ in the $\alpha\beta Z$ coordinate frame that maximize the orbit energy rate [Eq. (6)] are related to the velocity components according to Eqs. (A22) of the Appendix:

$$n_\alpha = -|v_\beta| \Big/ \sqrt{v_\beta^2 + \xi^2\left(v_\beta^2 + v_z^2\right)} \tag{26a}$$

$$n_\beta = \xi n_\alpha \tag{26b}$$

$$n_z = (v_z/v_\beta)n_\beta \tag{26c}$$

Equation (26c) indicates that the ratio of the optimal sail normal components in the plane of sky of the sun (the β–Z plane) is equal to the ratio of the corresponding velocity components. In other words, the optimal clock angle of the sail force is equal to the clock angle of the velocity vector.[1,11,22]

In Eq. (26a), the $\pm$ sign in Eq. (A22a) has been selected to ensure that $n_\alpha < 0$, so that the sail force points away from the sun (Fig. 1). The variable ξ in Eqs. (26a) and (26b) is defined in Eq. (A16):

$$\xi = \frac{-3v_\alpha v_\beta - v_\beta\sqrt{9v_\alpha^2 + 8\left(v_\beta^2 + v_z^2\right)}}{4\left(v_\beta^2 + v_z^2\right)} \tag{27}$$

where the choice of a $\pm$ sign has been made so that the component of sail acceleration along the velocity vector is maximized, as discussed in the Appendix. Equation (27) is equivalent to equations for the optimal cone angle in Refs. 1, 11, and 22.

The components of the sail acceleration in the $\alpha\beta Z$ frame are obtained from Eq. (1) and the components of the sail normal vector in Eqs. (26a–26c) as

$$\boldsymbol{\Delta} = \begin{bmatrix}\Delta_\alpha \\ \Delta_\beta \\ \Delta_z\end{bmatrix} = S_0 n_\alpha^2 \begin{bmatrix}n_\alpha \\ n_\beta \\ n_z\end{bmatrix} + \begin{bmatrix}g_p \\ 0 \\ 0\end{bmatrix} \tag{28}$$

where the fact has been used that the gravitational perturbation of the sun is in the α direction.

To obtain the disturbing acceleration components in the RTH frame of Eq. (16), one uses the expressions for the XYZ Cartesian components of the orbital radius and velocity vectors in terms of modified equinoctial elements from Ref. 41:

$$r_x = r[\cos L(1+\eta^2) + 2hk\sin L]/s^2 \tag{29a}$$

$$r_y = r[\sin L(1-\eta^2) + 2hk\cos L]/s^2 \tag{29b}$$

$$r_z = 2r(h\sin L - k\cos L)/s^2 \tag{29c}$$

where s^2 is defined in Eq. (19) and

$$\eta^2 \equiv h^2 - k^2 \tag{30}$$

The Cartesian velocity components are

$$v_x = -\sqrt{\mu/p}[(\sin L + g)(\eta^2+1) - 2hk(\cos L + f)]/s^2 \tag{31a}$$

$$v_y = -\sqrt{\mu/p}[(\cos L + f)(\eta^2-1) + 2hk(\sin L + g)]/s^2 \tag{31b}$$

$$v_z = 2\sqrt{\mu/p}[h(\cos L + f) + k(\sin L + g)]/s^2 \tag{31c}$$

The velocity components v_α and v_β in the rotating $\alpha\beta Z$ coordinate frame are calculated from the Cartesian components v_x and v_y of Eqs. (31a) and (31b) using

$$\begin{bmatrix}v_\alpha \\ v_\beta\end{bmatrix} = \begin{bmatrix}\cos\psi(t) & \sin\psi(t) \\ -\sin\psi(t) & \cos\psi(t)\end{bmatrix}\begin{bmatrix}v_x \\ v_y\end{bmatrix} \tag{32}$$

where the angle $\psi(t)$ in the rotation matrix in Eq. (32) is the celestial longitude of the sun, that is, the angle between the negative α axis and the x axis (Fig. 1). When a circular orbit is assumed for the Earth, this angle varies according to

$$\psi(t) = \omega_e t + \psi_0 \tag{33}$$

where ω_e is the (constant) orbital angular velocity of the earth about the sun and ψ_0 is the initial celestial longitude of the sun. The velocity component v_z (normal to the ecliptic plane) is the same in both the $\alpha\beta Z$ and XYZ frames and is given by Eq. (31c).

The procedure for calculating the disturbing acceleration components Δ_r, Δ_t, and Δ_h for use in the equations of motion (20–25) can be summarized as follows:

1) With use of the current values of the modified equinoctial elements $\{p, f, g, h, k, L\}$ at the current time t, calculate the Cartesian components r_x, r_y, and r_z of position and v_x, v_y, and v_z of velocity using Eqs. (29–31).

2) Calculate the $\alpha\beta$ components of velocity v_α and v_β using Eq. (32).

3) Calculate the sail normal unit vector components n_α, n_β, and n_z using Eqs. (26a–26c).

4) Calculate the disturbing acceleration components Δ_α, Δ_β, and Δ_z using Eq. (28).

5) Calculate the Cartesian components of the disturbing acceleration Δ_x, Δ_y, and Δ_z using the inverse (equal to the transpose) of the rotation matrix in Eq. (32) to yield

$$\boldsymbol{\Delta} = \Delta_x\hat{\boldsymbol{i}} + \Delta_y\hat{\boldsymbol{j}} + \Delta_z\hat{\boldsymbol{k}} \tag{34}$$

6) Calculate the Cartesian components of the unit vectors $\hat{\boldsymbol{r}}$, $\hat{\boldsymbol{t}}$, and $\hat{\boldsymbol{h}}$ using Eqs. (29–31) and the unit vector definitions Eqs. (13–15).

7) Calculate the RTH components of the disturbing acceleration using $\boldsymbol{\Delta}$ from step 5 and the units vectors from step 6 as

$$\Delta_r = \boldsymbol{\Delta}^T\hat{\boldsymbol{r}} \tag{35a}$$

$$\Delta_t = \boldsymbol{\Delta}^T\hat{\boldsymbol{t}} \tag{35b}$$

$$\Delta_h = \boldsymbol{\Delta}^T\hat{\boldsymbol{h}} \tag{35c}$$

Numerical results are presented in the next section, and a derivation of the control algorithm is given in the Appendix. However, some qualitative discussion is helpful about the geometry that maximizes the component of the sail acceleration along the velocity vector. Figure 2 shows the spacecraft heading away from the sun with a velocity component out of the ecliptic plane. In water sailing terminology, the spacecraft is running before the sunlight photon stream. The heavy solid line normal to $\boldsymbol{S}$ represents the flat sail. The solid vertical line shown is normal to the direction of the sun, and the sail acceleration vector $\boldsymbol{S}$ must point to the right of this line because the sun lies to the left. The dashed line is normal to the velocity vector $\boldsymbol{v}$. For the sail acceleration to cause an increase in the orbital energy, the component of $\boldsymbol{S}$ along $\boldsymbol{v}$ must be positive [Eq. (6)]. The direction of $\boldsymbol{S}$ shown provides a positive component of sail acceleration along the velocity vector.

One might think that aligning the sail acceleration vector with the velocity vector would maximize the amount of sail acceleration along the velocity, but the geometry shown in Fig. 2 actually provides a larger component of $\boldsymbol{S}$ along $\boldsymbol{v}$. This is because the magnitude of $\boldsymbol{S}$ decreases as the square of the cosine of the angle it makes with the ecliptic plane and is, therefore, fairly constant for small variations out of the ecliptic. The component of $\boldsymbol{S}$ along $\boldsymbol{v}$, however, varies as the cosine of the angle between them. Thus, the component of $\boldsymbol{S}$ along $\boldsymbol{v}$ is maximized by having $\boldsymbol{S}$ closer to the ecliptic plane than $\boldsymbol{v}$, as shown in Fig. 2. The optimal orientation is derived in the Appendix.

Figure 3 shows the spacecraft heading toward the sun with a velocity component out of the ecliptic plane. Here the spacecraft is tacking into the sunlight photon stream. Even though the spacecraft is heading toward the sun, the sail can be oriented so that there is a

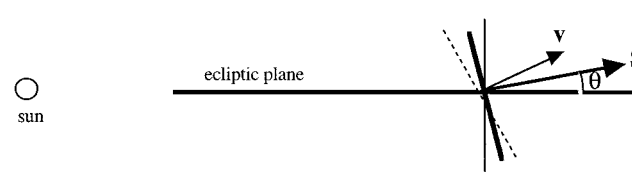

Fig. 2 Geometry normal to ecliptic plane with motion away from sun.

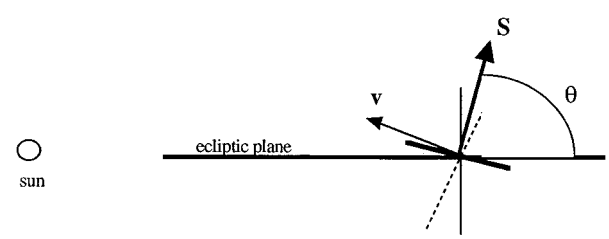

Fig. 3 Geometry normal to ecliptic plane with motion toward sun.

positive component of $\boldsymbol{S}$ along $\boldsymbol{v}$, as shown in Fig. 3. To achieve this, the sail acceleration must have a very large out-of-ecliptic component, as shown, so that the sail force clock angle is equal to that of the velocity vector, as required by Eq. (26c).

Figure 4 displays the geometry of $\boldsymbol{S}$ and $\boldsymbol{v}$ in the ecliptic plane. As can be seen, the sail acceleration has a positive component along the velocity vector at all points on the orbit except at the point where the velocity vector points directly toward the sun (at the very top of the orbit in Fig. 4). At that point, the best that can be done is to direct the sail acceleration normal to the velocity vector (and the sun direction) resulting in the instantaneous orbital energy rate due to the sail being zero. Any other sail orientation would provide a negative orbital energy rate. This is the only point in the orbit at which the sail is feathered.

The sail acceleration direction shown can be explained using Eq. (A3) of the Appendix, which indicates that the orbital energy rate has the same algebraic sign as

$$\boldsymbol{n}^T\boldsymbol{v} = n_\alpha v_\alpha + n_\beta v_\beta + n_z v_z \tag{36}$$

Because the sail acceleration $\boldsymbol{S}$ (and, hence, the sail normal $\boldsymbol{n}$) must be directed away from the sun, $n_\alpha < 0$. To maintain a positive orbital energy rate, n_β must have the same sign as v_β and n_z the same sign as v_z. In addition, when v_α is positive (upper half of the orbit in Fig. 4), the magnitude of n_β becomes large to offset the negative value of $n_\alpha v_\alpha$ in Eq. (36). By contrast, when v_α is negative (lower half of orbit in Fig. 4), the value of $n_\alpha v_\alpha$ is positive, and the magnitude of n_β becomes small, allowing the sail acceleration to be directed primarily along the velocity vector. This provides a large rate of increase of the orbital energy due to the sail.

Numerical Results

The sail acceleration control algorithm described is incorporated into the equations of motion (20–25). These equations are numerically integrated using the package ODE.[43] This package uses a modified difference form of the Adams predictor–corrector integration formulas with local extrapolation. The integration was performed in double precision on an IBM RS/6000 J30 with absolute and relative errors of 10^{-12}.

The initial orbit is taken to be a geosynchronous transfer orbit based on a standard Ariane 5 GTO. The initial perigee altitude is 600 km, the apogee occurs at local noon, and the inclination with respect to the equator is 7 deg. Two starting dates were used: northern hemisphere summer solstice and winter solstice. The reference plane used is the ecliptic.

Figure 5 shows the geometry for a deployment at winter solstice. The equatorial plane of the Earth is inclined with respect to the ecliptic plane by an angle of 23 deg (a rounded value of the obliquity of the ecliptic). The plane of the GTO is inclined with respect to the equatorial plane by 7 deg, with the apogee at local noon, as shown. Therefore the plane of the GTO is inclined with respect to the ecliptic at winter solstice by 16 deg, as shown.

Figure 6 shows the geometry for a deployment at summer solstice. The plane of the GTO is inclined with respect to the equatorial plane by 7 deg, with the apogee at local noon, as shown. Therefore, the plane of the GTO is inclined with respect to the ecliptic at summer solstice by 30 deg, as shown. Table 1 shows the classical orbital elements for these two sets of initial conditions and 1 distance unit (DU) = 6378 km.

Four values of sail acceleration are compared: 0.32, 0.43. 0.70, and 0.93 mm/s^2. The times required to achieve escape energy are shown in Table 2. In all cases, escape occurs, with the escape times ranging from approximately 4 to 11 months for the levels of sail accelerations considered. As seen, the solar gravitational perturbation effect is small (maximum less than 4%), with no apparent trend

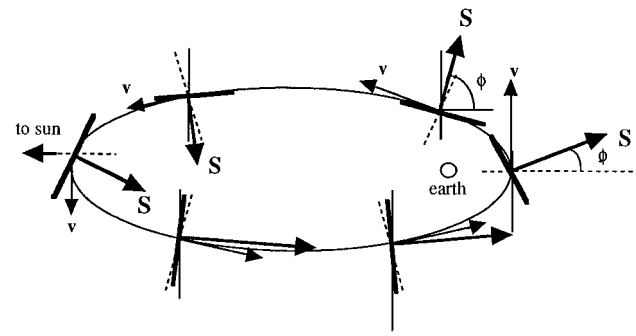

Fig. 4 Directions of velocity vectors and sail accelerations in the ecliptic plane.

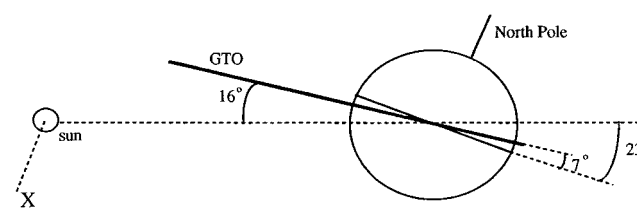

Fig. 5 Orbital geometry for winter solstice deployment.

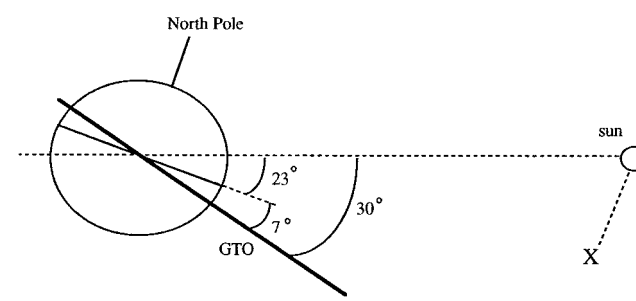

Fig. 6 Orbital geometry for summer solstice deployment.

Table 1 Initial orbital elements

Initial orbital elements	Winter solstice	Summer solstice
a, DU	3.852	3.852
e	0.716	0.716
i, deg	16	30
Ω, deg	180	180
ω, deg	270	90
f, deg	0	0

Table 2 Times to escape

Sail acceleration, mm/s^2	Time of year for deployment (solstice)	Time to escape with solar gravity, days	Time to escape no solar gravity, days	Effect of solar gravity on escape time, ±days
0.32	Summer	328	339	−11
0.32	Winter	325	327	−2
0.43	Summer	264	259	+5
0.43	Winter	252	258	−6
0.70	Summer	167	163	+4
0.70	Winter	168	162	+6
0.93	Summer	117	119	−2
0.93	Winter	122	120	+2

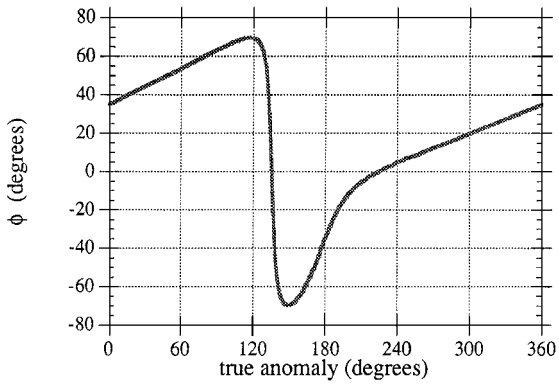

Fig. 7 Time history of the angle ϕ on the first orbit.

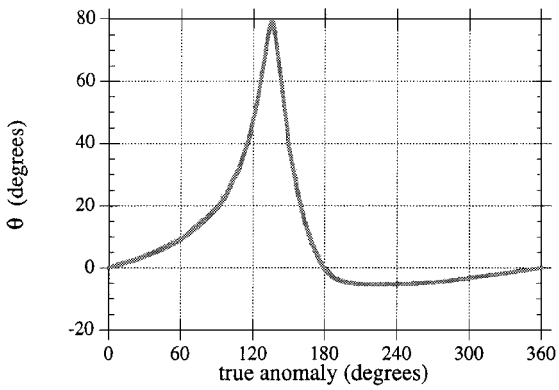

Fig. 8 Time history of the angle θ on the first orbit.

for increasing or decreasing the escape time. The effect of different time of year of deployment is similarly small.

Sail angles over the first orbit are shown in Figs. 7 and 8. The sail angle ϕ (in the ecliptic plane as shown in Fig. 4) is calculated using

$$\phi = \tan^{-1}(n_\beta / n_\alpha) \tag{37}$$

Figure 7 displays the sail angle ϕ in degrees for the $i = 16$ deg (with respect to the ecliptic) winter deployment. Note that, at the point where the spacecraft is heading directly toward the sun, the angle ϕ rapidly changes from a large positive value to a large negative value. This value is less than 90 deg because there is also an out-of-ecliptic component of sail acceleration.

Figure 8 displays the sail angle θ (out of the ecliptic plane) as shown in Fig. 3 and calculated using

$$\theta = \sin^{-1}(n_z) \tag{38}$$

Near the point in the orbit where the spacecraft is heading directly toward the sun, the control algorithm prescribes a large value of θ (sail angle out of the ecliptic plane) because 1) the sail is close to feathered ($n_\alpha \approx 0$) and 2) the value of n_β is small because the value of v_β is small [Eqs. (26b) and (27)]. Therefore, the value of n_z is close to 1. However, the magnitude of the sail acceleration in this situation is relatively small, and constraining the angle θ should produce only small degradation in performance.

Conclusions

An efficient algorithm has been derived and implemented to continuously orient the sail in three dimensions to maximize the instantaneous rate of change of the total orbital energy. When started in a GTO, escape trajectories of several months duration are successfully obtained for several sail acceleration magnitudes. Modified equinoctial elements provide a convenient means of handling the transition from elliptic to hyperbolic orbits. The time to escape is highly dependent on the sail acceleration magnitude but relatively independent of the time of year of deployment and the effect of solar gravitational perturbation.

The escape trajectories determined are known to be near-minimum-time trajectories for the order of magnitude of sail acceleration considered. They utilize a simple sail orientation control strategy and illustrate the feasibility of Earth escape using a solar sail.

Appendix: Optimal Sail Angles

In the Appendix, the control law that maximizes the component of the sail acceleration along the instantaneous velocity vector is derived. In the rotating $\alpha\beta Z$ coordinate frame shown in Fig. 1, the unit normal to the sail $\boldsymbol{n}$ has components

$$\boldsymbol{n}^T = [n_\alpha \quad n_\beta \quad n_z] \tag{A1}$$

Note that $n_\alpha < 0$ so that the sail force points away from the sun.

The sail acceleration can be represented as in Eq. (1),

$$\boldsymbol{S} = S_0(\boldsymbol{n}^T \hat{\boldsymbol{\alpha}})^2 \boldsymbol{n} \tag{A2}$$

To orient the sail to maximize the component of the sail acceleration along the velocity vector, one seeks to maximize $\boldsymbol{S}^T \boldsymbol{v}$. When Eq. (A2) is used,

$$\boldsymbol{S}^T \boldsymbol{v} = S_0(\boldsymbol{n}^T \hat{\boldsymbol{\alpha}})^2 \boldsymbol{n}^T \boldsymbol{v} \tag{A3}$$

The optimal sail orientation problem can then be posed as a constrained parameter optimization problem, namely, to maximize

$$H = S_0(\hat{\boldsymbol{\alpha}}^T \boldsymbol{n})^2 \boldsymbol{v}^T \boldsymbol{n} + \lambda(\boldsymbol{n}^T \boldsymbol{n} - 1) \tag{A4}$$

where λ is a Lagrange multiplier to adjoin the constraint that the vector $\boldsymbol{n}$ is a unit vector.

The first-order necessary condition for a maximum of H is given by

$$\frac{\partial H}{\partial \boldsymbol{n}} = \boldsymbol{0}^T \tag{A5}$$

which yields

$$2S_0(\hat{\boldsymbol{\alpha}}^T \boldsymbol{n})(\boldsymbol{v}^T \boldsymbol{n})\hat{\boldsymbol{\alpha}} + S_0(\hat{\boldsymbol{\alpha}}^T \boldsymbol{n})^2 \boldsymbol{v} + \lambda \boldsymbol{n} = \boldsymbol{0} \tag{A6}$$

with components in the $\alpha\beta Z$ coordinate frame,

$$\hat{\boldsymbol{\alpha}}^T = [1 \quad 0 \quad 0], \qquad \hat{\boldsymbol{\alpha}}^T \boldsymbol{n} = n_\alpha < 0 \tag{A7}$$

Equation (A6) represents three scalar equations in the $\alpha\beta Z$ frame,

$$2S_0 n_\alpha (n_\alpha v_\alpha + n_\beta v_\beta + n_z v_z) + S_0 n_\alpha^2 v_\alpha + \lambda n_\alpha = 0 \tag{A8a}$$

$$S_0 n_\alpha^2 v_\beta + \lambda n_\beta = 0 \tag{A8b}$$

$$S_0 n_\alpha^2 v_z + \lambda n_z = 0 \tag{A8c}$$

When Eqs. (A8b) and (A8c) are solved for λ,

$$\lambda = -S_0 n_\alpha^2 v_\beta / n_\beta = -S_0 n_\alpha^2 v_z / n_z \tag{A9}$$

Thus, if $n_\alpha \neq 0$ (the sail is not feathered),

$$n_z / n_\beta = v_z / v_\beta \tag{A10}$$

Equation (A10) indicates that the ratio of the sail normal components in the plane of sky of the sun (the β–Z plane) must be equal to the ratio of the corresponding velocity components. In other words, the optimal clock angle of the sail force is equal to the clock angle of the velocity vector.

From Eq. (A8a), either $n_\alpha = 0$ (the sail is feathered), or one divides by by $3S_0 n_\alpha^2$ and uses Eq. (A9) to obtain

$$3v_\alpha + 2(n_\beta / n_\alpha)v_\beta + 2(n_z / n_\alpha)v_z - (n_\alpha / n_\beta)v_\beta = 0 \tag{A11}$$

However, when Eq. (A10) is used,

$$n_z/n_\alpha = (n_z/n_\beta)(n_\beta/n_\alpha) = (v_z/v_\beta)(n_\beta/n_\alpha) \tag{A12}$$

If one defines

$$\xi \equiv n_\beta/n_\alpha \tag{A13}$$

and multiplies Eq. (A11) by ξv_β, the result is

$$3\xi v_\alpha v_\beta + 2\xi^2 v_\beta^2 + 2\xi^2 v_z^2 - v_\beta = 0 \tag{A14}$$

Collecting terms, one has a quadratic equation in ξ,

$$2\left(v_\beta^2 + v_z^2\right)\xi^2 + 3v_\alpha v_\beta \xi - v_\beta^2 = 0 \tag{A15}$$

which has solutions

$$\xi = \frac{-3v_\alpha v_\beta \pm v_\beta\sqrt{9v_\alpha^2 + 8\left(v_\beta^2 + v_z^2\right)}}{4\left(v_\beta^2 + v_z^2\right)} \tag{A16}$$

To resolve the $\pm$ sign, one needs to determine which sign maximizes the dot product of the sail acceleration and the velocity given in Eq. (A3). First rewrite Eq. (A3) as

$$\boldsymbol{S}^T\boldsymbol{v} = S_0 n_\alpha^2(n_\alpha v_\alpha + n_\beta v_\beta + n_z v_z) \tag{A17}$$

and divide by $S_0 n_\alpha^3$ and use Eqs. (A10) and (A13) to yield

$$\frac{\boldsymbol{S}^T\boldsymbol{v}}{\left(S_0 n_\alpha^3\right)} = v_\alpha + \xi\frac{\left(v_\beta^2 + v_z^2\right)}{v_\beta} \tag{A18}$$

However, from Eq. (A16),

$$\xi\left(v_\beta^2 + v_z^2\right)\Big/ v_\beta = -\tfrac{3}{4}v_\alpha \pm \tfrac{1}{4}\sqrt{9v_\alpha^2 + 8\left(v_\beta^2 + v_z^2\right)} \tag{A19}$$

Substituting Eq. (A19) into Eq. (A18) yields

$$\frac{\boldsymbol{S}^T\boldsymbol{v}}{\left(S_0 n_\alpha^3\right)} = \frac{1}{4}v_\alpha \pm \frac{1}{4}\sqrt{9v_\alpha^2 + 8\left(v_\beta^2 + v_z^2\right)} \tag{A20}$$

and because $n_\alpha < 0$, the left-hand side of Eq. (A20) is minimized ($\boldsymbol{S}^T\boldsymbol{v}$ is maximized) if the minus sign is used. This choice of sign in Eq. (27) guarantees that a maximum of $\boldsymbol{S}^T\boldsymbol{v}$ is achieved.

Using the result in Eq. (A10) and the definition in Eq. (A13), and the constraint that $\boldsymbol{n}$ is a unit vector,

$$n_\alpha^2 + n_\beta^2 + n_z^2 = 1 \tag{A21}$$

one determines the following expressions for the required components of $\boldsymbol{n}$:

$$n_\alpha = \pm v_\beta\Big/\sqrt{v_\beta^2 + \xi^2\left(v_\beta^2 + v_z^2\right)} \tag{A22a}$$

$$n_\beta = \xi n_\alpha \tag{A22b}$$

$$n_z = (v_z/v_\beta)n_\beta \tag{A22c}$$

where the $\pm$ sign in Eq. (22a) must be chosen so that $n_\alpha < 0$, that is, the sign is negative if v_β is positive and vice versa. This is accomplished by writing the numerator as $-|v_\beta|$, as is done in Eq. (26a) in the main text.

Acknowledgment

The research described in this paper was carried out for the Jet Propulsion Laboratory, California Institute of Technology, under contract with NASA.

References

[1]McInnes, C. R., *Solar Sailing: Technology, Dynamics and Mission Applications*, Springer-Praxis Series in Space Science and Technology, Springer-Verlag, Berlin, 1999.

[2]Tsiolkovsky, K. E., *Extension of Man into Outer Space*, 1921.

[3]Tsiolkovsky, K. E., *Symposium Jet Propulsion*, No. 2, United Scientific and Technical Presses (NTI), 1936.

[4]Tsander, K., *From a Scientific Heritage*, NASA Technical Translation TTF-541, 1967.

[5]Cotter, Y. P., "Solar Sailing," Sandia Corp. Research Colloquium, Rept. SCR-78, TID 4500, Albuquerque, NM, April 1959.

[6]Cavoti, C. R., "Numerical Solutions on the Astronautical Problem of Thrust Vector Control for Optimum Solar Sail Transfer," General Electric Co., Paper 2627-62, Valley Forge, PA, 13–18 Nov. 1962.

[7]Sands, N., "Escape from Planetary Gravitational Fields by Use of Solar Sails," *American Rocket Society Journal*, Vol. 31, 1961, pp. 527–531.

[8]Fimple, W. R., "Generalized Three-Dimensional Trajectory Analysis of Planetary Escape by Solar Sail," *American Rocket Society Journal*, Vol. 32, 1962, pp. 883–887.

[9]Zhukov, A. N., and Lebedev, V. N., "Variational Problem of Transfer Between Heliocentric Orbits by Means of a Solar Sail," *Cosmic Research*, Vol. 2, 1964, pp. 41–44.

[10]MacNeal, R. H., Hedgepeth, J. M., and Schuerch, H. U., "Heliogyro Solar Sailer Summary Report," NASA CR-1329, June 1969.

[11]Sauer, C. G., Jr., "Optimum Solar Sail Interplanetary Trajectories," AIAA Paper 76-0792, Aug. 1976.

[12]Wright, J., and Warmke, J., "Solar Sailing Mission Applications," American Astronautics Society, AAS Paper 76-808, Aug. 1976.

[13]Uphoff, C., "Escape from Elliptic Orbits by Solar Sail," Jet Propulsion Lab., Interoffice Memorandum, California Inst. of Technology, Pasadena, CA, March 1977.

[14]Sackett, L. L., and Edelbaum, T. N., "Optimal Solar Sail Spiral to Escape," AAS/AIAA Astrodynamics Conf., Sept. 1977.

[15]Green, A. J., "Optimal Escape Trajectory from a High Earth Orbit by Use of Solar Radiation Pressure," M. S. Thesis, Rept. T-652, Dept. of Aeronautics and Astronautics, Massachusetts Inst. of Technology, Cambridge, MA, 1977.

[16]Van der Ha, J. C., "The Attainability of the Heavenly Bodies with the Aid of Solar Sail," German Society for Aeronautics and Astronautics, DGLR Paper 80-012, March 1980.

[17]Jayaraman, T. S., "Time-Optimal Orbit Transfer Trajectory for Solar Sail Spacecraft," *Journal of Guidance and Control*, Vol. 3, No. 6, Nov.–Dec. 1980, pp. 536–542.

[18]Wood, L. J., Bauer, T. P., and Zondervan, K. P., "Comment on 'Time-Optimal Orbit Transfer Trajectory for Solar Sail Spacecraft,"' *Journal of Guidance, Control, and Dynamics*, Vol. 5, No. 2, March–April 1982, pp. 221–224.

[19]Friedman, L., *Starsailing–Solar Sails and Interstellar Travel*, Wiley, New York, 1988.

[20]Fekete, T. A., "Trajectory Design for Solar Sailing from Low Earth Orbit to the Moon," M.S. Thesis, Dept. of Aeronautics and Astronautics, Massachusetts Inst. of Technology, Cambridge, MA, Sept. 1991.

[21]Ocampo, C. A., and Rosborough, G. W., "Solar Sail Trajectories Near the Sun–Earth L_1 Point," *Advances in the Astronautical Sciences*, Vol. 76, Pt. 2, 1991, pp. 1253–1272.

[22]Fekete, T. A., Sackett, L. L., and von Flotow, A. H., "Trajectory Design for Solar Sailing from Low-Earth Orbit to the Moon," *Advances in the Astronautical Sciences*, Vol. 79, Pt. 3, 1992, pp. 1083–1094.

[23]Wright, J. L., *Space Sailing*, Gordon and Breach, New York, 1992.

[24]Subba Rao, P. V., and Ramanan, R. V., "Optimum Rendezvous Transfer between Coplanar Heliocentric Elliptic Orbits Using Solar Sail," *Journal of Guidance, Control, and Dynamics*, Vol. 15, No. 6, 1992, pp. 1507–1509.

[25]Sun, H., and Bryson, A. E., Jr., "Minimum Time Solar Sailing from Geosynchronous Orbit to the Sun–Earth L_2 Point," AIAA Paper 92-4657, Aug. 1992.

[26]Eguchi, S., Ishii, N., and Matsuo, H., "Guidance Strategies for Solar Sails to the Moon," *Advances in the Astronautical Sciences*, Vol. 85, Pt. 2, 1993, pp. 1419–1433.

[27]Leipold, M. E., and Wagner, O., "Mercury Sun-Synchronous Polar Orbits Using Solar Sail Propulsion," *Journal of Guidance, Control, and Dynamics*, Vol. 19, No. 6, 1996, pp. 1337–1341.

[28]Simon, K., and Zakharov, Y., "Optimization of Interplanetary Trajectories with Solar Sail Propulsion," *Space Technology*, Vol. 16, No. 5–6, 1996, pp. 381–385.

[29]Fieseler, P. D., "Method for Solar Sailing in a Low Earth Orbit," *Acta Astronautica*, Vol. 43, No. 9–10, 1998, pp. 531–541.

[30]Leipold, M., Garner, C. E., Freeland, R., Herrmann, A., Noca, M., Pagel, G., Sebolt, W., Sprague, G., and Unckenbold, W., "ODISSEE—a Proposal for Demonstration of a Solar Sail in Earth Orbit," *Acta Astronautica*, Vol. 45, No. 4, 1998, pp. 557–566.

[31] Sauer, C. G., Jr., "Solar Sail Trajectories for Solar Polar and Interstellar Probe Missions," *Advances in the Astronautical Sciences*, Vol. 103, Pt. 1, 1999, pp. 547–562.

[32] Rauwolf, G. A., and Friedlander, A., "Near-Optimal Solar Sail Trajectories Generated by a Genetic Algorithm," *Advances in the Astronautical Sciences*, Vol. 103, Pt 1, 1999, pp. 489–505.

[33] Cichan, T., and Melton, R. G., "Optimal Trajectories for Non-Ideal Solar Sails," *Advances in the Astronautical Sciences*, Vol. 109, Pt. 3, 2001, pp. 2381–2391.

[34] Colasurdo, G., and Casalino, L., "Optimal Control Law for Interplanetary Trajectories with Solar Sail," *Advances in the Astronautical Sciences*, Vol. 109, Pt. 3, 2001, pp. 2357–2368.

[35] Hughes, G. W., and McInnes, C. R., "Solar Sail Hybrid Trajectory Optimization," *Advances in the Astronautical Sciences*, Vol. 109, Pt. 3, 2001, pp. 2369–2379.

[36] Macdonald, M., and McInnes, C. R., "Analytic Control Laws for Near-Optimal Geocentric Solar Sail Transfers," *Advances in the Astronautical Sciences*, Vol. 109, Pt. 3, 2001, pp. 2393–2411.

[37] Otten, M., and McInnes, C. R., "Near Minimum-Time Trajectories for Solar Sails," *Journal of Guidance, Control, and Dynamics*, Vol. 24, No. 3, May–June 2001, pp. 632–634.

[38] Hughes, G. W., and McInnes, C. R., "Solar Sail Hybrid Trajectory Optimization for Non-Keplerian Orbit Transfers," *Journal of Guidance, Control, and Dynamics*, Vol. 25, No. 3, May–June 2002, pp. 602–604.

[39] Battin, R. H., *An Introduction to the Mathematics and Methods of Astrodynamics*, AIAA Education Series, AIAA, New York, 1987, Sec. 8.4.

[40] Hartmann, J. W., "Escape from Earth Using a Solar Sail," Dept. of Aeronautical and Astronautical Engineering, Final Rept. for AAE 493 Independent Study, Univ. of Illinois, Urbana-Champaign, IL, Feb. 2003.

[41] Betts, J. T., "Optimal Interplanetary Orbit Transfers by Direct Transcription," *Journal of Astronautical Sciences*, Vol. 42, No. 3, 1994, pp. 247–268.

[42] Walker, M. J. H., Ireland, B., and Owens, J., "A Set of Modified Equinoctial Orbit Elements," *Celestial Mechanics*, Vol. 36, 1985, pp. 409–419.

[43] Shampine, L. F., and Gordon, M. K., *Computer Solution of Ordinary Differential Equations: The Initial Value Problem*, W. H. Freeman., San Francisco, 1975, Chap. 10.